Langmuir

Article

pubs.acs.org/Langmuir

Structure and Properties of Cholesterol-based Hydrogelators with Varying Hydrophilic Terminals: Biocompatibility and Development of Antibacterial Soft Nanocomposites

Sounak Dutta, Tanmoy Kar, Deep Mandal, and Prasanta Kumar Das*

Department of Biological Chemistry, Indian Association for the Cultivation of Science Jadavpur, Kolkata −700 032, India

Supporting Information

ABSTRACT: The present work demonstrates a rational designing and synthesis of cholesterol-based amino acid containing hydrogelators with the aim to improve the biocompatibility of these amphiphilic molecules. A thorough structure−property correlation of these hydrogelators was carried out by varying the hydrophilic terminal from a neutral amine to a quaternized ammonium chloride. The amphiphiles having a cationic polar head as the hydrophilic domain and cholesterol as the hydrophobic unit showed better water gelation efficiency (minimum gelation concentration (MGC) ∼0.9−3.1%, w/v) than the analogous free amines. Presumably, the additional ionic interactions for the quaternized amphiphiles might have played the crucial role in gelation as counterions also got involved in hydrogen bonding with solvent molecules. Hence, the attainment of desired hydrophilic−lipophilic balance (HLB) of hydrophobic cholesterol in combination with the appropriate hydrophilic terminal led to the development of efficient hydrogels. Microscopic investigations revealed the formation of various supramolecular morphologies of hydrogels due to the variation in the molecular structure of the amphiphile. Spectroscopic investigations showed the involvement of hydrogen-bonding, hydrophobic, and $\pi-\pi$ interactions in the self-assembled gelation. Importantly, biocompatibility of all the cholesterol-based hydrogelators tested against human hepatic cancer derived HepG2 cells showed increased cell viability than the previously reported alkyl-chain-based amphiphilic hydrogelators. In order to incorporate broad spectrum antibacterial properties, silver nanoparticles (AgNPs) were synthesized in situ within the hydrogels using sunlight. The amphiphile−AgNP soft nanocomposite exhibited notable bactericidal property against both Gram-positive and Gram-negative bacteria.

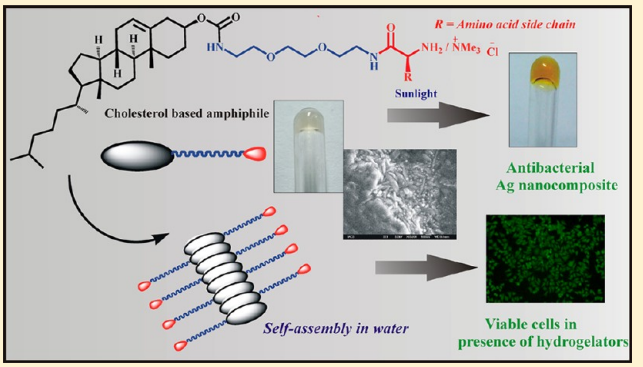

INTRODUCTION

Hydrogels are gaining unremitting importance because of their ever-expanding applications across scientific disciplines from advanced materials[1−6] to food processing to biomedicine.[7,8] Self-assembly of small molecules has been the prime aspect of supramolecular gelation that leads to the formation of soft materials such as hydrogels.[9−13] Incessant efforts are continuously on the rise for developing such soft materials with superior properties and desired applications such as drug delivery and controlled release,[14−16] tissue engineering,[17−19] pollutant capture,[20] enzyme immobilization matrices,[21,22] and many others.[23−31] Hydrogels have earned much interest particularly for biological applications simply because of their ability to imbibe water. Although, a large number of small molecules have been studied for self-assembled gelation in water, a constant advancement of this inventory is very important considering its potential applications. Ideally, a hydrogelator needs an optimum balance between hydrophobicity and hydrophilicity that would lead to self-assembled gelation.[31] In this regard, amphiphiles are always preferred as gelator molecules due to their intrinsic self-assembling ability. A large number of hydrogelators with varying functional motifs have been reported in the recent past that were used for diverse applications. However, to utilize them as biomaterials or in preparing/modifying biomedicinal implants, the prime challenge faced by chemists is to render them biocompatible.

A simple strategy to improve the biocompatibility of an amphiphilic gelator could be the inclusion of a biologically relevant molecule/precursor as one of its segments (either hydrophobic or hydrophilic). Cholesterol is known for its abundance and importance in biological systems, and amphiphiles composed of a cholesterol moiety are expected to show augmented biocompatibility. The steroidal backbone of cholesterol is a suitable option as the hydrophobic domain of the gelator.[25−27] Self-assembly of cholesterol-based molecules has been investigated previously including the host−guest chemistry of cholesterol and cyclodextrins.[32] However, most of the gelators designed using cholesterol have resulted in gelation of organic solvents.[25−27,33−37] Development of cholesterol-

Received: September 25, 2012
Revised: December 4, 2012

   dx.doi.org/10.1021/la3038389 | Langmuir XXXX, XXX, XXX−XXX

Chart 1. Structures of Cholesterol-based Amphiphiles

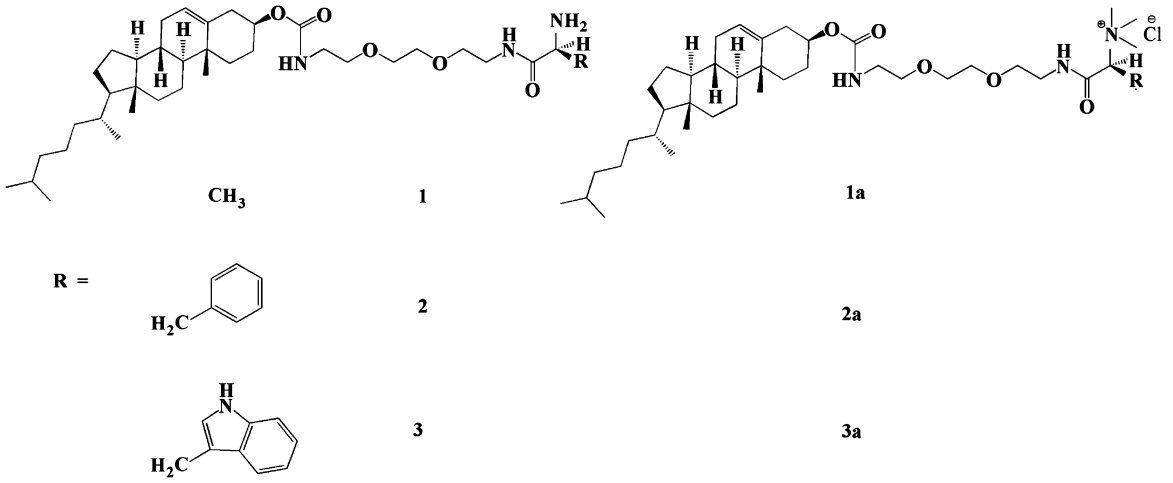

based functional hydrogels with structure−property correlation along with its cytocompatibility has not received due attention.

At the same time, the other crucial issue that's needs parallel attention during the development of self-assembled hydrogels is their ability to resist microbial infection. Biomedicinal implants induced infection in patients is a common phenomenon. Apart from a few examples, supramolecular gels are themselves inefficient in killing bacteria.[38−41] Inclusion of external bactericidal agents or synthesized in situ like silver nanoparticles (AgNPs) within self-assembled systems would increase the bactericidal property, and thereby, a superior soft nanohybrid will be developed.[42,43] Therefore, designing a biocompatible hydrogelator with a possible chance of accommodating an external antibacterial agent would be of great significance.

Herein, we report cholesterol-based hydrogelators comprising different amino acids linked by an oxyethylene spacer with a varying hydrophilic terminal (from free amine to quaternized trimethyl ammonium chlorides, Chart 1). The quaternized salts (**1a**−**3a**) exhibited better hydrogelation efficiency (minimum gelation concentration (MGC) = 0.9−3.1%, w/v) compared to the analogous amines (**1**−**3**). Spectroscopic and microscopic characterizations were carried out in detail to understand different driving forces involved in self-assembled hydrogelation. The amphiphilic hydrogelators showed significant viability toward mammalian cells. Also, hydrogelators **1** and **2** with a free amine at the terminal were used for in situ synthesis of AgNPs from $AgNO_3$ using sunlight, and the synthesized nanoparticles were stabilized within the supramolecular hydrogels. Although the cholesterol moiety is not directly involved in synthesis or stabilization of the AgNPs, the amine group present at the terminal of the gelators assisted in the stabilization of the nanoparticles. Soft nanocomposites AgNP−**1** and AgNP−**2** exhibited excellent bacteria killing ability against both Gram-positive and Gram-negative bacteria.

EXPERIMENTAL SECTION

Materials. Silica gel of 60−120 mesh, L-tryptophan, L-alanine, L-phenylalanine, *N*, *N*-dicyclohexylcarbodiimide (DCC), 4-*N*, *N*-(dimethylamino) pyridine (DMAP), 1-hydroxybenzotriazole (HOBT), Boc anhydride, trifluoroacetic acid (TFA), iodomethane, solvents, and all other reagents were procured from SRL, India. Water used throughout the study was Milli-Q water. Thin-layer chromatography was performed on precoated silica gel 60-F_{254} plates of Merck. $CDCl_3$ and other deuteriated solvents for NMR and Fourier transform IR (FTIR), uranyl acetate, cholesteryl chloroformate, 2,2′-(ethylenedioxy)bis(ethylamine), and Amberlite Ira-400 chloride ion exchange resins were obtained from Aldrich Chemical Co. Reagents required for preparing the nutrient broth culture medium such as peptone, yeast extract, and agar powder were purchased from Himedia Chemical Company, India. The LIVE/DEAD BacLight bacterial viability kit and LIVE/DEAD viability kit (L-3224) for mammalian cells were purchased from Molecular Probes, Invitrogen Chemical Company. High glucose Dulbecco's modified eagle medium (DMEM), heat inactivated fetal bovine serum (FBS), and trypsin−EDTA (0.05%) were purchased from Invitrogen. Penicillin−streptomycin and 3-(4,5-dimethyl-2-thiazolyl)-2,5-diphenyl-2H-tetrazolium bromide (MTT) were obtained from Sigma−Aldrich Chemical Co. ^{1}H NMR spectra were recorded in an AVANCE 500 MHz (Bruker) spectrometer. Mass spectrometry (MS) data were acquired by electron spray ionization (ESI) technique on a Q-tof-micro quadruple mass spectrometer (Micromass). Elemental analyses were performed on Perkin−Elmer 2400 CHN analyzer. UV−vis spectra were taken in a Perkin−Elmer lamda 25 spectrophotometer. Bath sonication was performed with a Telsonic ultrasonics bath sonicator. A Sorvall RC 6 and Sorvall RC 90 were used for centrifugation and ultracentrifugation, respectively.

Synthetic Procedure. All amphiphiles (**1**−**3**, **1a**−**3a**, Chart 1) were synthesized and characterized following the general principles of peptide chemistry described earlier.[31] Cholesteryl chloroformate was coupled with one end of 2,2′-(ethylenedioxy)bis(ethylamine) in dry dichloromethane (DCM) using a catalytic amount of dry triethylamine (Scheme S1, Supporting Information). The DCM solution of the cholesteryl chloroformate was added dropwise to the diamine solution under cold condition (0−5 °C). After complete addition, the solution was stirred for 8 h and then washed with water and brine to remove the excess base and the excess diamine. The DCM part was evaporated on a rotary evaporator, and solid product was obtained. The product was purified using column chromatography with chloroform−methanol as the eluent. The other end of the amine was coupled with Boc-protected L-amino acids using DCC and a catalytic amount of DMAP in the presence of HOBT. Boc-protected amide was then purified through column chromatography using 60−120 mesh silica gel and acetone−hexane as the eluent. The Boc-group was deprotected using TFA in dry DCM. After 2 h of stirring, the solvents were removed on a rotary evaporator, and the mixture was taken in ethyl acetate. The ethyl acetate part was thoroughly washed with 10% aqueous sodium carbonate solution followed by brine to neutrality. The organic portion was dried over anhydrous sodium sulfate and concentrated to get the corresponding amines (**1**−**3**, Chart 1). The produced amines (1 equiv) were quaternized with excess iodomethane using anhydrous potassium carbonate (2.2 equiv) and a catalytic amount of 18-crown-6-ether in dry DMF for 2 h. The reaction mixtures were taken in ethyl acetate and washed with aqueous sodium

dx.doi.org/10.1021/la3038389 | *Langmuir* XXXX, XXX, XXX−XXX

thiosulphate and brine solution, respectively. The concentrated ethyl acetate parts were crystallized from methanol−ether to obtain solid quaternized iodides, which were then subjected to ion exchange on an Amberlite Ira-400 chloride ion exchange resin column to get the pure desired amphiphile (**1a**−**3a**). Overall yields were in the range 65−80%.

*^{1}H NMR of **1** (500 MHz, $CDCl_3$, 25 °C).* δ = 1.06−2.33 (m, 43H, cholestanyl, and 3H, alanine), 3.25−3.59 (m, 12H, oxyethylene), 3.92 (br, 1H, cholestanyl (C*H*−O(CO)), 4.47 (br, 1H, chiral proton of amino acid), 5.36 (s, 1H, olefinic cholestanyl), 8.12 (br, 1H, amide). Elemental analysis calcd (%) for $C_{37}H_{65}N_3O_5$: C, 70.32; H, 10.37; N, 6.65; found: C, 70.49; H, 10.53; N, 6.91. MS (ESI): *m*/*z* calcd for $C_{37}H_{65}N_3O_5$: 631.4924; found: 632.4997 [M^+ + 1].

*^{1}H NMR of **2** (500 MHz, $CDCl_3$, 25 °C).* δ = 0.66−2.00 (m, 43H, cholestanyl), 3.33−3.44 (m, 2H, CH_2Ph), 3.47−3.51 (t, 4H, oxyethylene), 3.52−3.60 (m, 8H, oxyethylene), 3.95 (br, 1H, cholestanyl (C*H*−O(CO)), 4.43 (br, 1H, chiral proton of amino acid), 5.34 (s, 1H, olefinic cholestanyl), 7.20−7.30 (m, 5H, aromatic). Elemental analysis calcd (%) for $C_{43}H_{69}N_3O_5$: C, 72.94; H, 9.82; N, 5.93; found: C, 72.51; H, 9.59; N, 5.74. MS (ESI): *m*/*z* calcd for $C_{43}H_{69}N_3O_5$: 707.5237; found: 708.5300 [M^+ + 1].

*^{1}H NMR of **3** (500 MHz, $CDCl_3$, 25 °C).* δ = 0.65−2.29 (m, 43H, cholestanyl), 2.68−2.77 (d, 2H, CH_2−indole), 3.05−3.48 (m, 12H, oxyethylene), 4.44 (s, 1H, cholestanyl (C*H*−O(CO)), 4.83 (br, 1H, chiral proton of amino acid), 5.32 (s, 1H, olefinic cholestanyl), 7.01−7.48 (m, 5H, aromatic), 8.57 (s, 1H, amide). Elemental analysis calcd (%) for $C_{45}H_{70}N_4O_5$: C, 72.35; H, 9.44; N, 7.50; found: C, 72.49; H, 9.62; N, 7.12. MS (ESI): *m*/*z* calcd for $C_{45}H_{70}N_4O_5$: 746.5346; found: 747.5391 [M^+ + 1].

*^{1}H NMR of **1a** (500 MHz, $CDCl_3$, 25 °C).* δ = 0.67−2.33 (m, 43H, cholestanyl, and 3H, alanine), 3.39 (s, 9H, N(CH_3)$_3$), 3.55 (t, 4H, oxyethylene), 3.57−3.68 (m, 8H, oxyethylene), 4.34 (br, 1H, cholestanyl (C*H*−O(CO)), 5.05 (br, 1H, chiral proton of amino acid), 5.35 (br, 1H, olefinic cholestanyl), 8.83 (s, 1H, amide). Elemental analysis calcd (%) for $C_{40}H_{72}N_3O_5Cl$: C, 71.17; H, 10.75; N, 6.23; found: C, 71.24; H, 10.53; N, 5.98. MS (ESI): *m*/*z* calcd for $C_{40}H_{72}N_3O_5^+$: 674.5466; found: 674.5472 [M^+].

*^{1}H NMR of **2a** (500 MHz, $CDCl_3$).* δ = 0.64−2.29 (m, 43H, cholestanyl), 3.06−3.20 (m, 2H, CH_2Ph), 3.28−3.46 (m, 12H, oxyethylene), 3.39 (s, 9H, N(CH_3)$_3$), 4.43 (m, 1H, cholestanyl (C*H*−O(CO)), 5.25 (br, 1H, chiral proton of amino acid), 5.32 (br, 1H, olefinic cholestanyl), 7.21−7.31 (m, 5H, aromatic), 8.89 (s, 1H, amide). Elemental analysis calcd (%) for $C_{46}H_{76}N_3O_5Cl$: C, 73.56; H, 10.20; N, 5.59; found: C, 73.12; H, 10.65; N, 5.71. MS (ESI): *m*/*z* calcd for $C_{46}H_{76}N_3O_5^+$: 750.5779; found: 750.5784 [M^+].

*^{1}H NMR of **3a** (500 MHz, $CDCl_3$, 25 °C).* δ = 0.66−2.49 (m, 43H, cholestanyl), 2.94−2.98 (m, 2H, CH_2−indole), 3.18−3.36 (m, 12 H, oxyethylene), 3.48 (s, 9H, N(CH_3)$_3$), 4.33 (br, 1H, cholestanyl (C*H*−O(CO)), 5.30 (br, 1H, chiral proton of amino acid), 5.35 (br, 1H, olefinic cholestanyl), 7.09−7.22 (m, 2H, aromatic), 7.36−7.39 (d, 1H, aromatic), 7.54−7.60 (m, 2H, aromatic), 8.88 (br, 1H, amide). Elemental analysis calcd (%) for $C_{48}H_{77}N_4O_5Cl$: C, 72.96; H, 9.82; N, 7.09; found: C, 72.67; H, 9.48; N, 7.35; MS (ESI): *m*/*z* calcd for $C_{48}H_{77}N_4O_5^+$: 789.5888; found: 789.5891 [M^+].

Preparation of Hydrogel. The required amounts of the compounds were added in 400 μL of water in a screw-capped vial with an internal diameter (i.d.) of 10 mm and slowly heated until the solid was completely dissolved. The solutions were then cooled to room temperature without any disturbance. After 1 h, the formation of gel was confirmed by stable to inversion of the glass vial.

Microscopy Studies. Field emission scanning electron microscopy (FESEM) was performed on a JEOL-6700F microscope. A piece of hydrogel was mounted on a glass slide and dried for a few hours under vacuum. A Au coating was employed for 90 s before imaging. Transmission electron microscopy (TEM) images were acquired on a JEOL JEM 2010 high-resolution microscope. For TEM images, 5 μL of solution (10 times more dilute than MGC) was placed on a 300 mesh carbon coated copper grid. The sample was negatively stained with 2% uranyl acetate solution (2 μL) and dried under vacuum for 4 h before imaging. A similar procedure was followed for the AgNP−amphiphile composite solution (before and after centrifugation/lyophilization).

Circular Dichroism Spectroscopy. Circular dichroism (CD) spectra of the aqueous solutions of **2**, **2a**, and **3a** at varying concentrations were recorded by using a quartz cuvette of 1 mm path length in a Jasco J-815 spectropolarimeter. Temperature-dependent CD spectra (for **3a**) were also recorded at a concentration of 0.05% w/v from 20 to 90 °C.

FTIR Measurements. FTIR measurements of gelators **2** and **3a** in $CHCl_3$ solution and in the gel state in D_2O were carried out in a Perkin−Elmer spectrum 100 FTIR spectrometer using KBr and CaF_2 windows, respectively, with 1 mm Teflon spacers at their MGC.

Fluorescence Spectroscopy. The emission spectra of 8-anilino-1-naphthalenesulfonic acid (ANS) in varying concentrations of amphiphiles were recorded on a Varian Cary eclipse luminescence spectrometer. The probe molecules (ANS) were added to the aqueous solutions of amphiphiles at varying concentrations at room temperature. An ANS stock solution was prepared in MeOH, and from this super stock solution, the required amount of ANS solutions was added to gelators so that the final concentration of ANS solution was 1×10^{-5} M. The solution was excited at λ_{max} = 360 nm. The emission and excitation slit widths were 10 nm.

X-ray Diffraction. X-ray diffraction (XRD) measurements were taken in a Seifert XRD 3000P diffractometer, and the source was Cu Kα radiation (α = 0.15406 nm) with a voltage and current of 40 kV and 30 mA, respectively. Gels of **2** and **3a** were mounted on the glass slide and dried under vacuum. The xerogel was scanned from 1° to 40°.

NMR Experiments. Amphiphile **3a** was dissolved in D_2O (1% w/v), and temperature-dependent NMR was acquired from room temperature to 80 °C. In the case of NMR study using varying solvent proportion, initially, amphiphile **3a** was dissolved in DMSO-d_6 (1% w/v), and an NMR spectrum was taken. Subsequently, samples containing 10%, 20%, and 30% water were prepared (keeping the total solvent volume and amount of gelator constant), and their NMR spectra were acquired.

In Situ Synthesis of AgNPs. Amphiphiles **1** and **2** (Chart 1) were used for in situ synthesis of AgNPs. Hydrogels (400 μL) of the corresponding amines were prepared in accordance with the MGC (Table 1). To the hydrogel, 50 μL of $AgNO_3$ solution was added to maintain a gelator/$AgNO_3$ concentration of 10:1. In the case of **1**, the final gelator concentration was 75 mM, and the $AgNO_3$ concentrtion was ∼7.5 mM. In the case of **2**, the gelator concentration was 50.6 mM, and that of $AgNO_3$ was ∼5 mM. The mixture was kept in bright sunlight, and after 5 min, a change in color from colorless to yellow was noted. UV−vis spectra confirmed the synthesis of AgNPs. The solution containing nanoparticles was centrifuged at 30 000 rpm. The pellet was washed twice with Milli-Q water to remove excess silver ions and amphiphiles. The final pellet was lyophilized to get the nanocomposite powder. This powder was dispersed in water and used for antibacterial study.

Table 1. Minimum Gelation Concentration (MGC) of Amphiphiles

amphiphile	MGC (% w/v)
1	5.3
2	4.0
3	ins[a]
1a	3.1
2a	1.5
3a	0.9

[a]ins: insoluble.

Microorganisms and Culture Conditions. The in vitro antimicrobial activity of the nanocomposites was investigated against both Gram-positive and Gram-negative bacteria. The nutrient broth medium containing peptone (5 g) and yeast extract (3 g) in 1 L of

dx.doi.org/10.1021/la3038389 | *Langmuir* XXXX, XXX, XXX−XXX

sterile distilled water at pH 7.0 was used as a liquid medium, and nutrient agar (peptone (5 g), yeast extract (3 g), and agar (15 g) in 1 L of sterile distilled water at pH 7.0) was used as a solid medium in all antibacterial experiments. All the bacteria were procured from the Institute of Microbial Technology, Chandigarh, India. The stock solutions of the nanocomposites as well as the required dilutions were made using autoclaved sterile water. For all the bacteria, a representative single colony was picked up with a wire loop, and that loopful of culture was spread on a nutrient agar slant to give single colonies and incubated at 37 °C for 24 h. These fresh overnight cultures of all the bacteria were diluted as required to give a working concentration in the range 10^6–10^9 colony forming units (cfu)/mL before each experiment.

Antibacterial Studies. Minimum inhibitory concentrations (MICs) of the AgNP-based soft nanocomposites were estimated by the liquid broth method and the spread plate method.[42] The MIC was measured using a series of test tubes containing the composites (5–150 μg/mL) in 5 mL of liquid medium. The diluted microbial culture was added to each test tube in identical concentrations to obtain the working concentration for *Escherichia coli*, 3.75×10^7 to 7.5×10^7 cfu/mL; for *Bacillus subtilis*, 7.5×10^7 to 1×10^8 cfu/mL; for *Staphylococcus aureus*, 5×10^6 to 7.5×10^6 cfu/mL; and for *Pseudomonas aeruginosa*, 9×10^7 to 1.2×10^8 cfu/mL. All the test tubes were then incubated at 37 °C for 24 h. The optical density of all the solutions was measured before and after incubation at 650 nm. Liquid medium containing microorganisms was used as a positive control. For the spread plate method, 50 μL from each tube was spread onto nutrient agar plates inside the laminar hood. Finally, plates were incubated for 24 h at 37 °C and the viable cells were counted. The experiments were performed in triplicate and were repeated twice.

Fluorescence Microscopy Study. The LIVE/DEAD BacLight bacterial viability kit was used to examine bacterial cell viability under a fluorescence microscope. The kit contains a mixture of two nucleic acid binding stains, specifically referred to as SYTO 9 and propidium iodide. The kit was stored at −20 °C in the dark; it was taken out and thawed at room temperature just prior to the assay. *E. coli* (3.75×10^7 to 7.5×10^7 cfu/mL) was treated with AgNP–**2** above MIC and also untreated cells were taken in a centrifuge tube. The mixtures were centrifuged at 5000 rpm for 5 min at 4 °C. Then, the media was removed completely, and the cells were redispersed in 0.9 wt % saline. Finally, 3 μL of the BacLight dye mixture was added and incubated in the dark at room temperature for 15–20 min. After incubation, 5 μL of the solution mixture was mounted over microscope slides, which were then air-dried and viewed under the light microscope (BX61, Olympus) using an excitation filter of BP460–495 nm and a band absorbance filter covering wavelength below 505 nm.

Cell Cultures. Human hepatic cancer derived HepG2 cells were obtained from the National Center for Cell Science (NCCS), Pune (India), and maintained in DMEM supplemented with 10% FBS, 100 mg/L streptomycin, and 100 IU/mL penicillin. Cells were grown in 25 mL cell culture flasks and incubated at 37 °C in a humidified atmosphere of 5% CO_2 to approximately 70–80% confluence. Media was changed after every 2–3 days, and subculture was performed every 7 days. After 7 days, the media was removed to eliminate the dead cells. Next, the adherent cells were detached from the surface of the culture flask by trypsinization. Cells were now in the exponential phase of growth for checking the toxicity of the amphiphiles.

Cytotoxicity Assay. Cell viability of amphiphiles was assessed by the microculture MTT reduction assay.[42] This assay is based on the reduction of a soluble tetrazolium salt by mitochondrial dehydrogenase of the viable cells to a water-insoluble colored product, formazan. The amount of formazan formed can be measured spectrophotometrically after dissolution of the dye in DMSO. The activity of the enzyme and the amount of the formazan produced is proportional to the number of cells alive. Reduction of the absorbance value can be attributed to the killing of the cells or inhibition of cell proliferation by the composites. Cells were seeded at a density 15 000 cells per well in a 96-well microtiter plate for 18–24 h before the assay. Stock solutions of all the amphiphiles were prepared in water. Sequential dilutions of these stock solutions were done during the experiment to vary the concentrations (5–100 μg/mL) in the microtiter plate. The cells were incubated for 6 h at 37 °C under 5% CO_2. Then, 15 μL of the MTT stock solution (5 mg/mL) in phosphate-buffered saline (PBS) was added to the above mixture, and the cells were further incubated for 3 h. The precipitated formazan was dissolved thoroughly in DMSO, and the absorbance at 570 nm was measured using a BioTek ELISA reader. The number of surviving cells was expressed as percent viability = (A_{570}(treated cells) − background/A_{570}(untreated cells) − background) × 100.

Fluorescence Microscopy Study to Check Cell Viability. The LIVE/DEAD viability/cytotoxicity kit for mammalian cells was used to examine cell viability under a fluorescence microscope. The kit contains a mixture of two nucleic acid binding stains, specifically referred to as Calcein AM (component A) and ethidium homodimer-1 (EthD-1, component B). The acetomethoxy derivative of Calcein (Calcein AM) has the ability to pass through the cell membrane. After its transportation into the cell, the esterase enzyme present in live cells removes the acetoxy group. This form of the compound then intercalates with the DNA and results in an enhancement of fluorescence, and a bright green color can be observed. This binding occurs in the presence of the esterase enzyme, which is present only in live cells. Ethidium homodimer can only pass through damaged cell membranes; thus, it gets incorporated only into dead cells. It does not require any enzyme and shows red fluorescence upon binding with DNA in the dead cells. The kit was stored at −20 °C in the dark, which is taken out and thawed at room temperature just prior to assay. A portion (4 μL) of the supplied 2 mM EthD-1 stock solution (component B) was added to 2 mL of sterile, tissue culture-grade PBS, and the mixture was vortexed to ensure thorough mixing. This gave an approximately 4 μM EthD-1 solution. A portion (1 μL) of the supplied 4 mM calcein AM stock solution (component A) was then added to the 2 mL of EthD-1 solution and vortexed. The resulting approximately 2 μM calcein AM and 4 μM EthD-1 working solution was then added directly (500 μL) to HepG2 cells treated with the amphiphile having a concentration of 50 μg/mL and incubated for 24 h. After incubation with the fluorescent dye, the cells were observed under the Olympus IX51 inverted microscope using an excitation filter of BP460–495 nm and a band absorbance filter covering wavelength below 505 nm. The bright green color resulting from the enhanced fluorescence of DNA-intercalated calcein indicated the presence of viable cells. When the images were taken using the excitation filter BP530–550 and a band absorbance filter covering wavelength below 570 nm, negligible red fluorescence was observed, which confirmed the absence of dead cells rather ensured the abundance of live cells.

RESULTS AND DISCUSSION

Designing small molecules that can entrap solvents resulting in the formation of supramolecular gels has fascinated chemists for long. In recent past, efforts have been made to include "task-specific functionalities" in the molecular structures of hydrogelators to widen their prospect in different disciplines including biomedicinal applications.[1−18] In order to improve the biocompatibility and biodegradability, gelator structure is often tethered with a biomolecular precursor.[44,45] In previous work, we have developed several amino acid based amphiphilic hydrogelators that comprised long alkyl chain as the hydrophobic unit.[31,42] However, most of these gelators failed to show significant viability toward mammalian cells particularly at a longer time scale. It is believed that the lipophilic chain penetrates the cell membrane resulting in the death of cells.[46,47] In this context, we have made efforts to improve the biocompatibility of amphiphilic hydrogelators by varying the counterions at the hydrophilic end and also by introducing an amino acid moiety at the hydrophobic tail to reduce the penetration ability of the alkyl chain.[42,48] Instead of diminishing the lipophilic character of the alkyl tail, we thought of replacing the hydrophobic unit with a biologically relevant precursor such

dx.doi.org/10.1021/la3038389 | Langmuir XXXX, XXX, XXX–XXX

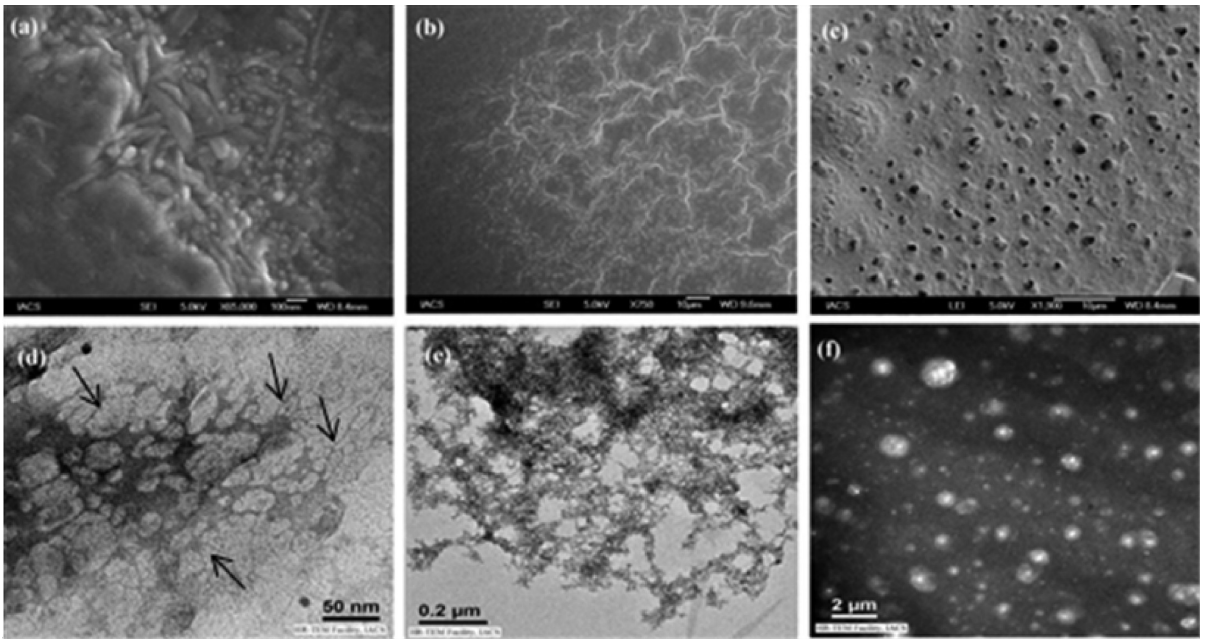

Figure 1. FESEM images of dried gel of (a) **2**, (b) **2a**, and (c) **3a** ; TEM images of dried gels of (d) **2** (arrows indicate the presence of thin fibers), (e) **2a**, and (f) **3a**.

as cholesterol. In the present work, we have exploited this steroidal unit as the hydrophobic moiety to develop amphiphilic hydrogelators with the objective of improving the cytocompatibility of the molecule.

Structure Correlation of the Amphiphilic Molecules with Their Gelation Properties. Cholesterol and the amino acid were linked together using an oxyethylene diamine spacer. The C terminal of the amino acid was connected to the spacer through an amide linkage, and the steroid moiety was tethered to the other end of oxyethylene diamine (Chart 1). Amphiphilic compounds were synthesized using L-alanine, L-phenylalanine, and L-tryptophan having a free primary amine at the N terminal (**1**−**3**, Chart 1). The synthetic procedures (Scheme S1, Supporting Information) are illustrated in the Experimental Section. We have initially used an aliphatic amino acid, L-alanine, with an amine at the polar head (**1**, Chart 1). This cholesterol-based amphiphilic compound showed weak hydrogelation ability with an MGC of 5.3% w/v (Table 1). It was apparent that the crucial balance between hydrophobicity and hydrophilicity for **1** was not optimum, which is essential for superior gelation. However, the presence of hydrogen-bonding units such as an amide, an oxyethylene spacer, and a free amine group might have facilitated the self-assembled gelation of **1** in water, although its MGC was high. Cholesterol possibly contributed toward the gelation through its hydrophobic interactions. The presence of an aromatic moiety is known to facilitate self-assembly of molecules in water through $\pi-\pi$ interaction.[31] With this comprehension, we used aromatic amino acids instead of L-alanine. In the case of the L-phenylalanine-based amine (**2**), gelation efficiency moderately improved as the MGC slightly decreased to 4.0% w/v (Table 1). This decrease in the MGC was presumably due to the additional $\pi-\pi$ interaction between the aromatic rings in **2**. Hence, an extended aromaticity possibly could result in more efficient hydrogelation for cholesterol based amphiphilic amine. We introduced the L-tryptophan amino acid (**3**) comprising an extended aromatic system (indole moiety). Surprisingly, free amine **3** was found to be insoluble in water. The amphiphile in combination of cholesterol and tryptophan linked by an oxyethylene diamine spacer might have lost the critical hydrophilic−lipophilic balance (HLB) required for even its solubilization in water.

Previously, we have observed that, in the case of long chain amphiphilic amino acid based compounds, modification of a primary amine to a quaternized ammonium chloride resulted in the formation of efficient hydrogelators.[48,49] Thus, to improve the hydrogelating efficiency of the present cholesterol-based amphiphiles, we transformed the primary amines to the corresponding quaternized trimethylammonium chloride salts (**1a**−**3a**, Chart 1) keeping all other functional moieties unaltered. In the case of the alanine-based quaternized amphiphile (**1a**, Chart 1), enhancement in the gelation efficiency was noted (MGC = 3.1% w/v, Table 1) compared to that was observed for the corresponding free amine, **1** (MGC = 5.3% w/v). In addition to the alteration of HLB, the ionic interactions also played a crucial role in gelation as the counterion got involved in hydrogen bonding with solvent molecules. The hydrogelation ability of this cholesterol-based alanine-containing quaternized amphiphile is noteworthy because the corresponding hydrophobic long alkyl chain (instead of cholesterol) quaternized amphiphile of alanine failed to exhibit any hydrogelation ability (as reported earlier).[50] This certainly points to the fact that the hydrophobic cholesterol moiety is responsible for self-aggregating interactions that facilitated the supramolecular hydrogelation. The quaternized ammonium chloride of phenylalanine (**2a**) showed even more efficient hydrogelation (MGC, 1.5% w/v, Table 1). Almost 2.7-fold improvement in the gelation efficiency in **2a** was observed with respect to the precursor free amine (**2**, MGC = 4.0% w/v). The additional effect of aromatic $\pi-\pi$ interaction along with the ionic interaction of the polar head further bolstered the self-assembled gelation. Strikingly, the quaternization of the tryptophan-containing cholesterol-based amphiphile (**3**) led to the development of the superior hydrogelators (**3a**)

dx.doi.org/10.1021/la3038389 | *Langmuir* XXXX, XXX, XXX−XXX

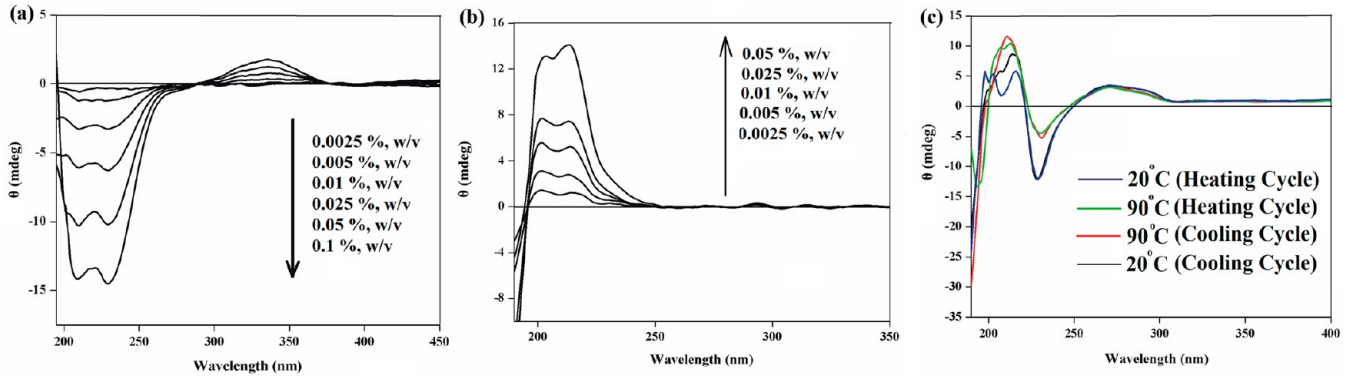

Figure 2. Concentration-dependent CD spectra of (a) **2**, (b) **2a**, and (c) temperature-dependent heating and cooling cycle for **3a** (0.05% w/v).

with a MGC of only 0.9% w/v (Table 1). Although free amine **3** was insoluble in water, quaternization of the same resulted in the formation of the most efficient hydrogelator, **3a**. The transformation of the primary amine to the quaternary ammonium headgroup resulted in the development of efficient gelators possibly due to the attainment of optimum HLB in the amphiphiles required for self-assembled gelation. Thus, the complementary effect of the cholesterol-based hydrophobic segment and the tailor-made hydrophilic end led to the development of efficient amphiphilic hydrogelators. In previous instances, the presence of an aromatic moiety was found to be a prerequisite for the hydrogelation of amphiphilic molecules having a long alkyl chain as the hydrophobic unit.[31,49,50] However, in the present case, the hydrophobic cholesterol could induce hydrogelation in presence of both aliphatic (**1** and **1a**) as well as aromatic amino acids (**2**, **2a**, and **3a**).

Gel-to-Sol Transition Temperature (T_{gel}). The gel-to-sol transition temperatures (T_{gel}) of all the hydrogels were measured at varying concentrations of gelators. Hydrogels were thermoreversible in nature, turning to sol when heated and again forming semisolid gels upon cooling down to room temperature. T_{gel} values of the hydrogels were between 45 and 60 °C at corresponding MGCs, which is quite similar to those reported for long alkyl chain based hydrogels (Figure S1, see the Supporting Information). Also, in concurrence with previous studies, T_{gel} values were found to increase with increasing concentration of gelators.[31]

Microscopy Studies. In order to find out the structural morphologies of the hydrogels at the self-assembled state, they were visualized through FESEM and TEM. Among the free amines, **2** was chosen as a representative for its better gelation ability. The FESEM image of **2** showed supramolecular networks comprising nanometer-sized fibrils. Individual fibers of ∼40 nm in thickness were entangled to form thicker fibers (Figure 1a). We also carried out microscopic investigation of hydrogels of quaternized salts **2a** and **3a** (once again chosen for their superior water gelation ability) to find out whether modification at the molecular level brought any changes in supramolecular self-assembly. The amphiphilic gelator **2a** featuring L-phenylalanine at the polar head exhibited supramolecular meshlike structures comprising fibers having a diameter of ∼1 μm and several micrometers in length. The supramolecular fibrils were interconnected with each other thereby forming a greater network (Figure 1b). However, in the case of **3a**, (L-tryptophan at the polar head), porous structures (or spherical voids) were observed in the self-assembled state in the corresponding FESEM image (Figure 1c) with pore diameters varying from 0.5 to 2 μm.[44] The zoomed image in TEM also shows similar voids within the supramolecular mesh of the self-assembled amphiphiles (Figure S2, Supporting Information). In a few reports, it was observed that modification of a particular polymeric molecule with cholesterol resulted in the formation of porous networks. Such a difference in supramolecular morphologies is quite intriguing and might be due to the change in the molecular architecture of the amphiphiles that modulated the self-assembling behavior of the cholesterol-based hydrogels. A similar difference in supramolecular architecture was also noted in TEM images of the corresponding hydrogels. The TEM image of **2** exhibited supramolecular structures that are interconnected with thin fibers (Figure 1d). The fibers are visible at the terminal of the supramolecular networks. Hydrogels of **2a** showed fibrillar meshlike morphology, while **3a** revealed spherical voids in the self-assembled state (Figure 1e,f). Self-association of the amphiphiles generally results in the formation of fibrillar or other supramolecular structures that entraps solvent molecules.[51] However, the combination of a cholesterol moiety as the hydrophobic unit and a quaternized ammonium group as the hydrophilic domain resulted in a supramolecular hydrogel of different self-assembling morphologies.

CD Spectroscopy. Gelation is a phenomenon that is visibly identified from the "stable to inversion" nature of the amphiphilic solution at MGC. However, self-association of these amphiphiles initiates at a much lower concentration, which transforms into higher order aggregates with increasing concentration of amphiphile resulting in the formation of gel at MGC. The nature of supramolecular aggregation that depends on the molecular structure of the amphiphile was investigated using CD spectroscopy. Hydrogelator **2** showed a negative cotton effect with double minima peaks at 208 and 228 nm (Figure 2a). These peaks became more prominent with the increase in the concentration of amphiphile from 0.0025% to 0.1% w/v. The observed nature of the CD spectrum with double minima is a characteristic of an α-helical structure of proteins.[52] Therefore, this α-helical type of arrangement of **2** in the self-assembled state led to the formation of fibril network structures that was observed in the corresponding microscopic images (Figure 1). Nevertheless, there was a positive peak with weak intensity at a longer wavelength (335 nm) in the CD spectra of **2**. This might be due to the n−π* transition involved with the amide bond of the amphiphile.[49] Interestingly, with modification of the amine to **2a**, the nature of supramolecular association was found to be different. The amphiphile showed positive cotton effects with two peaks at 203 and 213 nm

dx.doi.org/10.1021/la3038389 | Langmuir XXXX, XXX, XXX−XXX

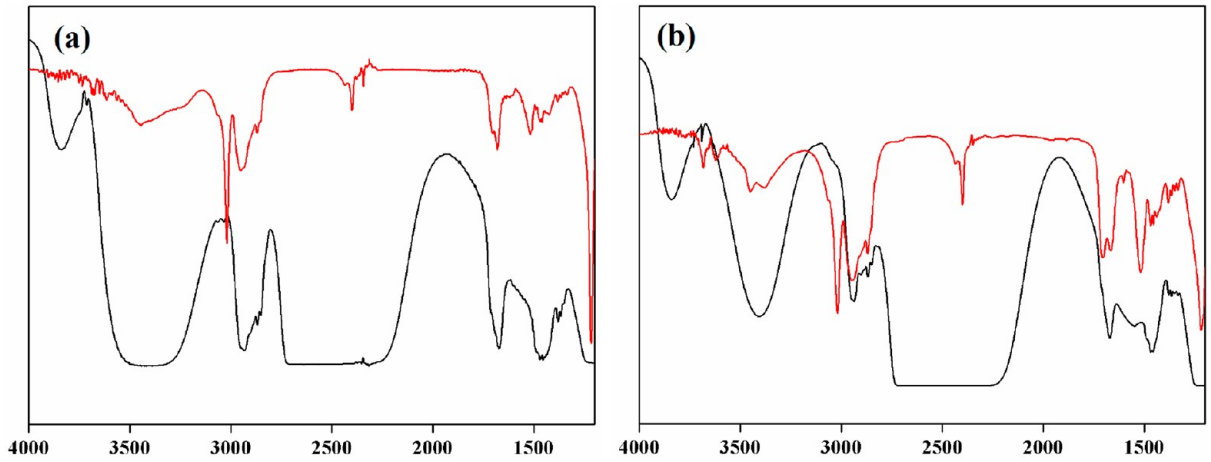

Figure 3. FTIR spectra of (a) **2** and (b) **3a**; (black line: gel state in D_2O; red line: sol state in $CHCl_3$).

(Figure 2b). In all the cases, higher ordered structures were formed from the association of individual amphiphiles that showed increase in the peak intensity with increasing gelator concentration.

The noncovalent supramolecular association of the self-assembled hydrogel was studied using temperature-dependent CD spectroscopy of **3a** (chosen for its superior hydrogelation ability). Initially, CD spectra of **3a** in water were acquired at 20 °C (with an amphiphile concentration of 0.05% w/v) (Figure 2c). A positive cotton effect in the amide absorption region (210 nm) was accompanied with a negative peak at 230 nm and a shoulder at longer wavelength (270 nm). This particular pattern of CD spectra is analogous to the β-sheet arrangement of the peptide backbone,[52] which has mostly dominated the self-assembly of gelator **3a**. Thus, a significant change in supramolecular packing of the molecules in the self-assembled state was observed with variation in the molecular structure of the amphiphiles. The CD spectrum of **3a** was further recorded at 90 °C at the same concentration. The nature of the peaks was similar to the spectra taken at 20 °C; however, the peak intensity notably decreased. Hence, at higher temperature, there was significant loss of the higher ordered aggregates that formed through the supramolecular association of the amphiphile. With lowering of temperature further to 20 °C, the self-assembly of the gelator molecule was restored as the observed CD spectrum almost matched with that of the initial spectra taken at 20 °C (Figure 2c). Temperature-dependent CD spectra clearly revealed the thermoreversible nature of the self-assembled hydrogels because of the noncovalent supramolecular assembly, the nature of which depends on the structure of amphiphile.

FTIR Spectra. FTIR spectroscopy is a powerful tool to elucidate noncovalent interactions, especially hydrogen bonding present within self-associated systems.[31] To find out the involvement of amide moieties toward hydrogen-bonding interactions in self-assembled gelation, FTIR spectra of **2** and **3a** (taken as representatives from both free amine and quaternized category as efficient gelators) were recorded in $CHCl_3$ (for sol) and D_2O (for gel state). It was observed that, in the sol state, the amide-I (carbonyl) stretching frequencies were at 1682 and 1699 cm^{-1} for **2** and **3a**, respectively (Figure 3a, b). However the same peaks were shifted to lower frequencies at 1670 and 1673 cm^{-1} for **2** and **3a**, respectively in D_2O (Figure 3a,b). Such a decrease in the amide-I stretching clearly indicates the presence of intermolecular hydrogen bonding within the amide moieties of the neighboring molecules. We also observed that the νN−H (amide A) stretching frequency appeared in the range 3440−3445 cm^{-1} in the nonself-assembled state in $CHCl_3$. However, at the gel state in D_2O, the corresponding peak appeared in the range 3405−3415 cm^{-1}. This decrease is also characteristic of hydrogen-bonded N−H stretching. Thus, hydrogen bonding is obviously playing the crucial role in the process of self-assembled hydrogelation.

Luminescence Studies. Hydrophobic interaction among the molecules is an important factor in the supramolecular association in particular for hydrogelation.[31] Involvement of hydrophobic interaction in the case of cholesterol-based amino acid containing gelators was investigated using an external hydrophobic fluorophore, ANS. We have doped ANS (1×10^{-5} M) in the aqueous solution of amphiphilic hydrogelators with varying concentration and noted the change in the nature of the fluorescence peak. We have taken amphiphiles **2** and **3a** as representative examples. In the case of both gelators, the emission peak of ANS increased initially with a blueshift (475 nm) with respect to native ANS (510 nm in water). In the case of **2**, the intensity of the ANS peak increased up to a concentration of 1% w/v, which is 4 times below the MGC (Figure S3a, Supporting Information). The increase in the fluorescence intensity of ANS can be attributed to the enhanced hydrophobicity in its microenvironment. Also, the increase in the emission intensity was accompanied with a further blueshift of the peak (~3 nm). With further increase in the concentration of **2**, the intensity of the ANS peak was decreased along with generation of an extra peak at a lower wavelength (395 nm). Similarly, in the case of **3a**, initially at very low concentration, the ANS peak appeared at 474 nm, the intensity of which increased with a blueshift (465 nm, Figure S3b, Supporting Information) up to an amphiphile concentration of 0.1% w/v (which is 9-fold lower than the MGC). Such characteristic behavior of ANS clearly indicates the participation of hydrophobic interaction during the self-assembly. The emission intensity notably decreased with increase in the concentration of **3a** with another shoulder peak appearing at lower wavelength. Thus, the gelation process of the amphiphiles seemed to undergo via an intermediate state of self-association at which ANS experienced maximum hydrophobicity. Molecules within the self-assembled hydrogel

dx.doi.org/10.1021/la3038389 | *Langmuir* XXXX, XXX, XXX−XXX

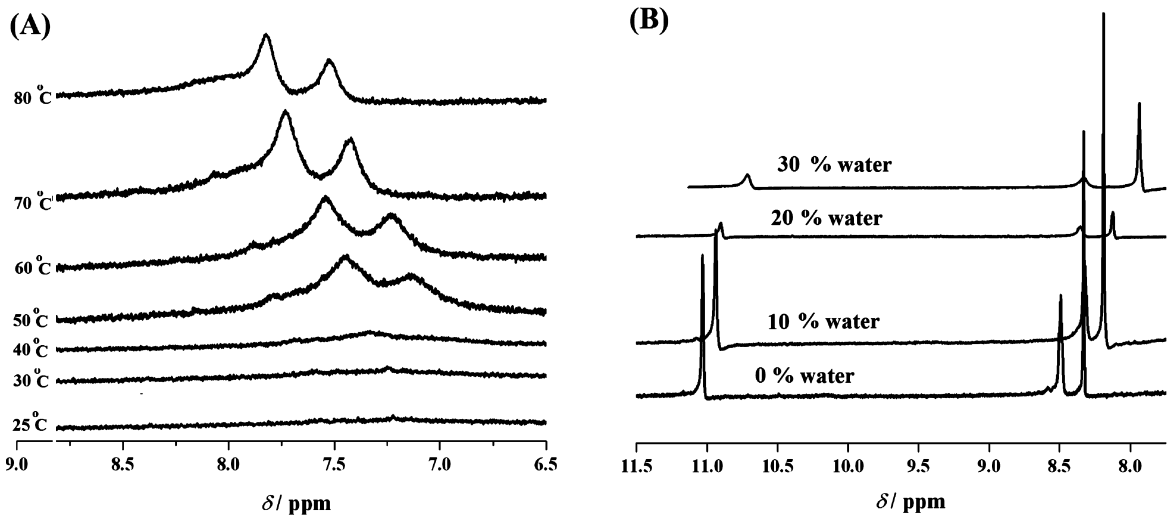

Figure 4. (A) ^{1}H NMR spectra of **3a** (1% w/v) in D_2O with varying temperature and (B) in DMSO-d_6 with increasing H_2O content.

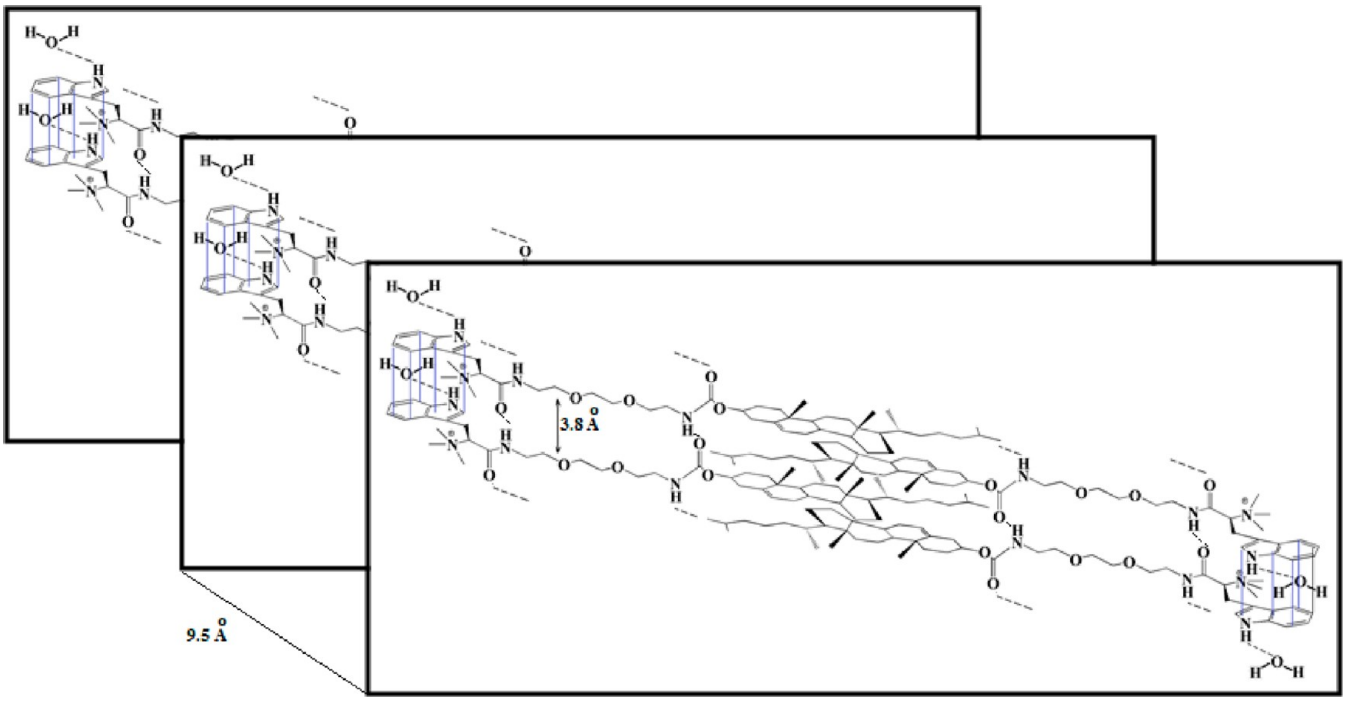

Figure 5. Pictorial representation of the plausible packing of cholesterol-based amphiphilic hydrogelator **3a** in the self-assembled state (counterions were not shown).

might have experienced a less hydrophobic environment compared to that of the intermediate state of gelation possibly due to the well-ordered network at the gel state. At higher concentrations of gelators, the splitting of the fluorescence peaks may be a result of anisotropic heterogeneity or formation of amphiphile bound ANS.[31,53]

NMR Spectroscopy. ^{1}H NMR experiments were performed to understand further the intermolecular interactions involved in the self-assembled gelation. In a temperature-dependent NMR study, ^{1}H NMR of **3a** (1% w/v) in D_2O hardly exhibited any peaks in the aromatic region at room temperature. However, with an increase in the temperature, the initially broad peak of aromatic protons appeared, which gradually transformed to a sharper peak at a higher δ value at 80 °C (which is much above the T_{gel} of the gelator) (Figure 4A). At 40 °C, broad peaks started to appear at δ 7.33 ppm that got shifted and separated to sharper peaks at 7.51 and 7.82 ppm at 80 °C (Figure 4A). This clearly indicates the involvement of the aromatic rings in supramolecular gelation. At the gel state (in D_2O), the aromatic rings are involved in a strong $\pi-\pi$ interaction. As a result, the protons are not in their characteristic spinning motion and could not exhibit sharp individual peaks in the NMR spectra being in the aggregated forms.[49] With an increase in temperature, the intermolecular noncovalent interactions get destroyed, and the amphiphile loses its gelation efficiency leading to the transformation from gel-to-sol where the protons showed their characteristic signals.

Similarly, participation of hydrogen-bonded interactions during gelation was studied through ^{1}H NMR experiments using 1% w/v **3a** in DMSO-d_6 with an increasing amount of

dx.doi.org/10.1021/la3038389 | Langmuir XXXX, XXX, XXX−XXX

water. Initially, the NMR of **3a** (1% w/v) was recorded in DMSO-d_6 where the amphiphile was in the nonself-assembled state. The indole N−H proton appeared at δ 11.03 ppm. Also in DMSO-d_6, amide protons showed characteristic sharp signals at 8.33 and 8.49 ppm, since there is no self-assembling and H bonding (Figure 4B). Water content in that system was then gradually increased up to 30%. In general, the signals of the NMR protons were broadened accompanied by a shift at lower δ value. At 30% water content, the indole N−H proton was observed at 10.73 ppm, and the amide protons were shifted to 7.99 and 8.32 ppm, respectively (Figure 4B). This upfield shift clearly suggests the involvement of indole N−H and amide protons in H bonding and also the contribution of the $\pi-\pi$ stacking interaction between the indole moiety to the self-aggregation of the amphiphiles in the gel state.[54] With an increase in water content, self-assembly initiated, which instigated the intermolecular packing of the molecules and other noncovalent interactions.

XRD. In order to get detailed insight toward the molecular packing of the amphiphiles in the self-assembled gel state, we have performed wide-angle XRD of dried gels of **2** and **3a**. The thin film of dried hydrogel **2** gave a peak at 2θ = 10.5° that corresponds to a d spacing of 8.42 Å. This is accompanied with another broad peak at 2θ = 21.2° that corresponds to a d spacing of 4.12 Å (Figure S4, Supporting Information). The peak at higher 2θ (21.2°) designates the intermolecular distance while the smaller 2θ (10.5°) was due to the spacing between two consecutive layers. Similar peaks were also observed in the xerogel of **3a**, where the distance between the two stacked layers was 9.5 Å (2θ = 9.39°) and that between the two amphiphiles was 3.8 Å (2θ = 23.33°) (Figure S4, Supporting Information and Figure 5).

An ordered arrangement of the cholesterol-based amino acid containing amphiphilic gelators at the self-assembled state can be suggested involving H-bonding, $\pi-\pi$ stacking, and hydrophobic interactions on the basis of the above-discussed spectroscopic and microscopic experiments (representative example is given for **3a** in Figure 5). The hydrophobic units were stacked on one another with the hydrophilic terminals stretched away on either side. H bonding between the amide groups of the alternate molecules and the indole N−H with H_2O facilitated the self-association of the amphiphiles. Additionally, $\pi-\pi$ stacking between the aromatic groups (in the case of **2**, **2a**, and **3a**) contributed toward the gelation phenomena (Figure 5). Individual molecules were oriented in a layer-by-layer fashion that developed the higher ordered packing in the three-dimensional network of the hydrogel.[52]

Cell Viability. The prime objective of choosing cholesterol as the hydrophobic moiety in designing amphiphilic hydrogelators was to ensure that these newly developed gelators have substantial biocompatibility. To this end, we have investigated the cell viability of these amphiphilic hydrogelators toward human hepatic cancer derived HepG2 cell line by MTT-based assay (details given in the Experimental Section). Encouragingly, all the hydrogelating amphiphiles showed significant biocompatibility after a 6 h incubation period. At a concentration of 5 μg mL^{-1}, more than 95% of the cells were found alive (Figure 6). With an increase in the concentration of the amphiphile, a gradual decrease in the biocompatibility was observed. However, even at a concentration of 100 μg mL^{-1}, 55−70% cell viability was noted (Figure 6). Amphiphiles at further higher concentration showed precipitation effects in the cell culture media and as a result could not be used for MTT

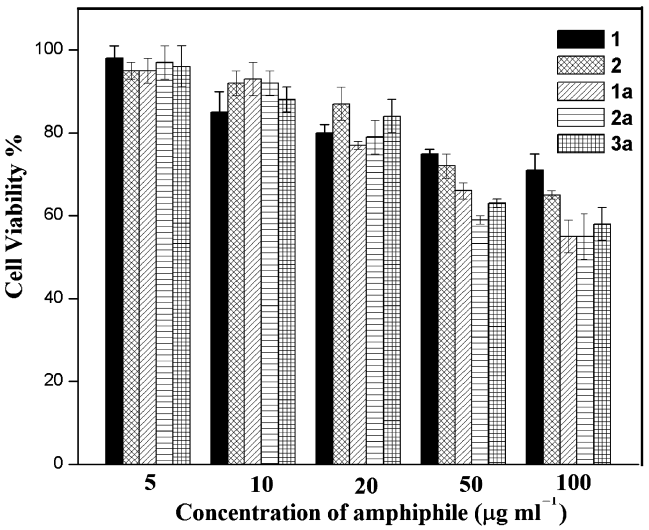

Figure 6. MTT-based % cell viability of HepG2 cells with varying concentration of amphiphilic hydrogelators (incubation period was 6 h).

experiments. The cationic gelators (**1a**−**3a**) exhibited slightly enhanced cytotoxicity compared to that of the neutral amines (**1**, **2**).

The positively charged amphiphiles obviously had an electrostatic interaction with the eukaryotic cell membrane comprising zwitterionic lipids such as phosphatidylcholine and sphingomyelin. However, at comparable concentrations, cholesterol-based amphiphilic gelators exhibited notably higher biocompatibility than the corresponding alkyl chain based amino acid containing hydrogelators previously studied (Figure S5, Supporting Information).The viability of cells in the presence of amphiphile **2** was also checked using the Live/Dead viability kit for mammalian cells. The bright green color resulting from the enhanced fluorescence of DNA-intercalated calcein indicated that most of the cells were alive. However, negligible red fluorescence confirmed the absence of dead cells. (Figure S6, Supporting Information). The hydrophobic long chain is presumed to play a crucial role in penetrating the cell membranes after favorable electrostatic interaction between the cell surface and the polar headgroup. However, by substituting the alkyl chain with cholesterol, the present hydrophobic unit is possibly less effective in disrupting the eukaryotic cell membrane. Moreover, the cholesterol-rich eukaryotic cell membranes presumably could impede the inclusion of an additional steroidal moiety at the cell surface. So, we have been successful in bringing down the cytotoxicity of hydrogelators by the inclusion of a cholesterol moiety in the amphiphile's structure. Thus, the rationally designed hydrogelators in the present study having significant cytocompatibility might be considered for the development of biomaterials/biomedicinal implants in future.

Synthesis of AgNPs within Hydrogels and Antibacterial Properties. Nosocomial infections are most common obstacles associated with the development of implants for biomedicinal use. In this context, many previously reported hydrogelators were not found to be intrinsically antimicrobial. However, a serious effort and attention is necessary to make them capable of killing microbes.[55−57] In this regard, recently, a few cationic amphiphilic hydrogelators have shown effective bactericidal property against Gram-positive bacteria; however,

dx.doi.org/10.1021/la3038389 | Langmuir XXXX, XXX, XXX−XXX

most of them were incapable to kill Gram-negative strains. On the contrary, those amphiphilic hydrogelators also did not exhibit substantial mammalian cell viability. In order to develop effective antibacterial as well as biocompatible soft materials, we used these cholesterol-based amphiphilic hydrogels for synthesis and stabilization of AgNPs (well-known antibacterial agents). Utilizing self-assembled systems for synthesis of metal nanoparticles (MNPs) has been an interesting subject of research in the recent past.[42,43,55,58−60] In fact, efforts have been concerted in developing gelator molecules with the ability to synthesize and/or stabilize MNPs within the hydrogel matrix so that the composite soft material can exhibit superior mechanical or biological properties.[42,43,55,58−60] Herein, we have synthesized AgNPs in situ within cholesterol-based hydrogels by using sunlight irradiation at physiological pH using $AgNO_3$ as the precursor. Sunlight-mediated AgNP synthesis is considered to be a green technique for preparation of AgNPs that does not involve the use of toxic chemicals or harmful UV irradiation.[60] Amphiphiles **1** and **2** were used for this purpose with an assumption that the terminal amine will provide additional stability to the synthesized AgNPs along with the supramolecular networks of the hydrogel.[59] The quaternized chloride salts (**1a−3a**) obviously could not be used for the synthesis of AgNPs from $AgNO_3$ due to the precipitation of AgCl. Hydrogels **1** and **2** were prepared at their MGCs (Table 1), and $AgNO_3$ was added to maintain a gelator/$AgNO_3$ concentration at 10:1. The hydrogels (after addition of $AgNO_3$) were kept in sunlight, and after 5 min, transformation of the colorless gel to yellow was observed. We monitored the AgNP formation through UV−vis absorbance of diluted aqueous solutions of the hydrogels. In the case of **1**, a broad peak around 420 nm was observed, while a relatively sharp peak at 418 nm for **2** indicated the formation of AgNPs (Figure S7, Supporting Information). Formation of AgNPs was also followed by TEM that revealed the presence of stabilized nanoparticles within the supramolecular network of hydrogel **2** (Figure 7a). Magnification of the same image showed monodisperse nanoparticles of an average diameter of 8 nm (Figure 7b).

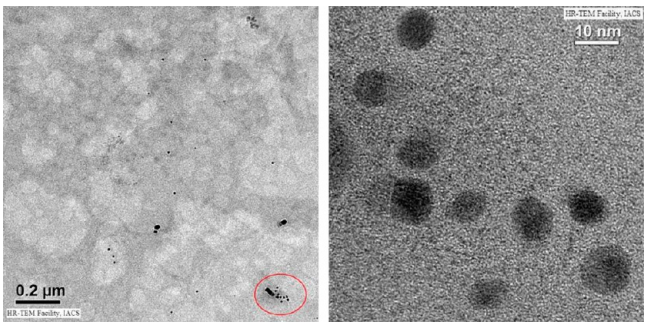

Figure 7. TEM images of (a) AgNPs synthesized within self-assemblies of hydrogelator **2**; (b) magnified image of AgNPs.

This AgNP hydrogel composite was centrifuged, and the pellet was washed twice with water to remove unreacted silver ions. It was then lyophilized and dispersed in water. The negatively stained TEM image of this dispersed nanocomposites showed similar sized nanoparticles within supramolecular fibrillar network (Figure S8, Supporting Information).

We tested the antibacterial activity of these nanocomposites through the broth dilution method against both Gram-positive and Gram-negative bacteria to determine its potentials in biomedicinal applications. The MIC (the lowest amphiphile concentration at which no viable bacterial cell is present) values for AgNP−**1** were 70 and 50 $\mu g\ mL^{-1}$ against Gram-positive bacteria *B. subtilis* and *S. aureus*, respectively (Table 2). The

Table 2. MIC of Soft Nanocomposites in $\mu g/mL$

	Gram-positive bacteria		Gram-negative bacteria	
nanocomposite	*B. subtilis*	*S. aureus*	*E. coli*	*K. aerogenes*
AgNP−**1**	70	50	100	75
AgNP−**2**	30	20	60	50

MIC values in the case of Gram-negative bacteria were a little higher (for *E. coli*, 100 $\mu g\ mL^{-1}$, and for *P. aeruginosa*, 75 $\mu g\ mL^{-1}$, Table 2). Interestingly, the soft nanocomposite AgNP−**2** exhibited better bactericidal property compared to that of AgNP−**1** having MIC values of 30 and 20 $\mu g\ mL^{-1}$ for Gram-positive *B. subtilis* and *S. aureus*, respectively, and MIC values of 60 and 50 $\mu g\ mL^{-1}$ for Gram-negative *E. coli* and *P. aeruginosa*, respectively (Table 2). It is well known that antibacterial activity of AgNPs is dependent on the shapes and size of the nanoparticles.[61] Here, also, the AgNPs were synthesized in a different supramolecular environment formed by hydrogelators **1** and **2**. Also, the UV absorbance spectrum of AgNP−**2** showed a sharp peak while that of AgNP−**1** showed a broader peak. This indicated a broad size distribution of nanoparticles in the case of AgNP−**1**, which possibly reduces its antibacterial efficacy. The killing ability of these soft composites against the Gram-negative bacteria is relatively weaker than that against the Gram-positive bacteria due to the presence of an extra layer of protection by lipopolysaccharide in addition to the peptidoglycan membrane for the former.[39,42,55]

Antibacterial activity was also investigated through the spread plate method. For this purpose, the same amount of bacterial cultures (*E. coli*) were added to test tubes containing AgNP−**2** (80 $\mu g\ mL^{-1}$, higher than the MIC value) and also in the absence of the nanocomposite (control). After 5−7 h incubation, 50 μL from each test tube was spread on agar plates and kept at 37 °C for 24 h. We observed that, in absence of the soft nanocomposite (the control plate), there was normal growth of bacteria. However, no viable bacterial cell was seen in the agar plate treated with AgNP−**2** (Figure S9, Supporting Information). Hence, the present AgNP−amphiphile composites exhibited broad spectrum antibacterial activity due to the bactericidal property of AgNPs.

We also studied the antibacterial activity of AgNP composites by fluorescence microscopy using the commercially available LIVE/DEAD BacLight bacterial viability kit. The kit is composed of two nucleic acid binding stains, known as SYTO 9 and propidium iodide. These dyes have different cell penetration properties as well as different spectral characteristics. SYTO 9 binds to the nucleic acid of both living and dead cells, while propidium iodide can only bind to the nucleic acid of dead cells. Consequently, all live cells show green fluorescence, and dead cells with compromised cell membranes appear red under the fluorescence microscope. Figure S10a (see the Supporting Information) showed the control image of *E. coli*, while Figure S10b showed the fluorescence images of the *E. coli* cells treated with AgNP−**2** (80 $\mu g/mL$) above their MIC values. All untreated bacterial cells exhibited green fluorescence

dx.doi.org/10.1021/la3038389 | *Langmuir* XXXX, XXX, XXX−XXX

(Figure S10a, Supporting Information), indicating that they were alive. However, the antimicrobial activity of the soft nanocomposite was further confirmed from the observed red fluorescence for bacterial cells treated with AgNP−**2** (Figure S10b, Supporting Information).

CONCLUSION

Cholesterol-based cationic and neutral hydrogelators comprising different amino acids (aliphatic and aromatic) were designed and synthesized. The amino acid at the polar head bearing cationic charge exhibited better gelation ability compared to the corresponding free amine containing amphiphiles. Different spectroscopic and microscopic techniques were employed to determine the involvement of different noncovalent driving forces such as intermolecular H-bonding, $\pi-\pi$ stacking, and hydrophobic interactions of cholesterol in the self-assembled gelation. Designing of amphiphilic hydrogelators using a cholesterol moiety as the hydrophobic segment was successfully achieved. A judicious combination of hydrophilic terminal with the cholesterol led to the development of efficient hydrogels. Importantly, cholesterol-based amphiphiles showed improved biocompatibility as compared to those having a long alkyl chain as the hydrophobic part. Thus, introducing a steroidal moiety can be an effective strategy for decreasing the cytotoxicity of the system. Also, these biocompatible hydrogels were transformed to antibacterial matrix by in situ synthesis of AgNPs. The soft nanocomposite showed broad spectrum antibacterial properties. Development of such soft materials with significant cell viability complemented by antibacterial property can be an effective step for designing smart biomaterials in future.

ASSOCIATED CONTENT

Supporting Information

Synthetic procedure of amphiphiles, T_{gel} of the amphiphilic gelators, TEM image of **3a**, luminescence spectra of ANS within self-assemblies of **2** and **3a**, XRD spectra of gels, cell viability of alkyl chain based hydrogelators, fluorescence live/dead images of HepG2, UV−vis spectra of AgNP, TEM image of AgNP−**2**, growth of *E. coli* on agar plates in the absence and presence of AgNP−**2**, and fluorescence images of control and AgNP−**2** treated bacteria. This material is available free of charge via the Internet at http://pubs.acs.org.

AUTHOR INFORMATION

Corresponding Author

*Fax: +(91)-33-24732805; e-mail: bcpkd@iacs.res.in.

Notes

The authors declare no competing financial interest.

ACKNOWLEDGMENTS

P.K.D. is thankful to Department of Science and Technology, India, (SR/S1/OC-25/2011) for financial assistance. S.D., T.K., and D.M. acknowledge Council of Scientific and Industrial Research, India, for research fellowships.

REFERENCES

(1) John, G.; Vemula, P. K. Design and Development of Soft Nanomaterials from Biobased Amphiphiles. *Soft Matter* **2006**, *2*, 909−914.

(2) van Bommel, K. J. C.; van der Pol, C.; Muizebelt, I.; Friggeri, A.; Heeres, A.; Meetsma, A.; Feringa, B. L.; van Esch, J. Responsive Cyclohexane-based Low-Molecular-Weight Hydrogelators with Modular Architecture. *Angew. Chem., Int. Ed.* **2004**, *43*, 1663−1667.

(3) Bernet, A.; Behr, M.; Schmidt, H.-W. Supramolecular Nanotube-based Fiber Mats by Self-Assembly of a Tailored Amphiphilic Low Molecular Weight Hydrogelator. *Soft Matter* **2011**, *7*, 1058−1065.

(4) Heeres, A.; van der Pol, C.; Stuart, M.; Friggeri, A.; Feringa, B. L.; van Esch, J. Orthogonal Self-Assembly of Low Molecular Weight Hydrogelators and Surfactants. *J. Am. Chem. Soc.* **2003**, *125*, 14252−14253.

(5) Verdejo, B.; Rodriguez-Llansola, F.; Escuder, B.; Miravet, J. F.; Ballester, P. Sodium and pH Responsive Hydrogel Formation by the Supramolecular System Calix[4]Pyrrole Derivative/Tetramethylammonium Cation. *Chem. Commun.* **2011**, *47*, 2017−2019.

(6) Banerjee, S.; Kandanelli, R.; Bhowmik, S.; Maitra, U. Self-Organization of Multiple Components in a Steroidal Hydrogel Matrix: Design, Construction and Studies on Novel Tunable Luminescent Gels and Xerogels. *Soft Matter* **2011**, *7*, 8207−8215.

(7) Bernet, A.; Behr, M.; Schmidt, H.-W. Supramolecular Hydrogels Based on Antimycobacterial Amphiphiles. *Soft Matter* **2012**, *8*, 4873−4876.

(8) Agrawal, S. K.; Sanabria-DeLong, N.; Bhatia, S. K.; Tew, G. N.; Bhatia, S. R. Energetics of Association in Poly(lactic acid)-based Hydrogels with Crystalline and Nanoparticle−Polymer Junctions. *Langmuir* **2010**, *26*, 17330−17338.

(9) Estroff, L. A.; Hamilton, A. D. Water Gelation by Small Organic Molecules. *Chem. Rev.* **2004**, *104*, 1201−1218.

(10) Roy, S.; Javid, N.; Frederix, P. W. J. M.; Lamprou, D. A.; Urquhart, A. J.; Hunt, N. T.; Halling, P. J.; Ulijn, R. V. Dramatic Specific-Ion Effect in Supramolecular Hydrogels. *Chem.—Eur. J.* **2012**, *18*, 11723−11731.

(11) Rodriguez-Llansola, F.; Escuder, B.; Hamley, I. W.; Hayes, W.; Miravet, J. F. Structural and Morphological Studies of the Dipeptide Based L-Pro-L-Val Organocatalytic Gels and Their Rheological Behavior. *Soft Matter* **2012**, *8*, 8865−8872.

(12) Lagadec, C. A.; Smith, D. K. Structure−Activity Effects in Peptide Self-Assembly and Gelation − Dendritic versus Linear Architectures. *Chem. Commun.* **2012**, *48*, 7817−7819.

(13) Pal, A.; Basit, H.; Sen, S.; Aswal, V. K.; Bhattacharya, S. Structure and Properties of Two Component Hydrogels Comprising Lithocholic Acid and Organic Amines. *J. Mater. Chem.* **2009**, *19*, 4325−4334.

(14) Barnard, A.; Posocco, P.; Pricl, S.; Calderon, M.; Haag, R.; Hwang, M. E.; Shum, V. W. T.; Pack, D. W.; Smith, D. K. Degradable Self-Assembling Dendrons for Gene Delivery: Experimental and Theoretical Insights into the Barriers to Cellular Uptake. *J. Am. Chem. Soc.* **2011**, *133*, 20288−20300.

(15) Boekhoven, J.; Koot, M.; Wezendonk, T. A.; Eelkema, R.; van Esch, J. H. A Self-Assembled Delivery Platform with Post-production Tunable Release Rate. *J. Am. Chem. Soc.* **2012**, *134*, 12908−12911.

(16) Jadhav, S. R.; Chiou, B. S.; Wood, D. F.; Hoffman, G. D.; Glenn, G. M.; John, G. Molecular Gels-based Controlled Release Devices for Pheromones. *Soft Matter* **2011**, *7*, 864−867.

(17) Lee, K. Y.; Mooney, D. J. Hydrogels for Tissue Engineering. *Chem. Rev.* **2001**, *101*, 1869−1880.

(18) Jayawarna, V.; Ali, M.; Jowitt, T. A.; Miller, A. F.; Saiani, A.; Gough, J. E.; Ulijn, R. V. Nanostructured Hydrogels for Three-Dimensional Cell Culture Through Self-Assembly of Fluorenylmethoxycarbonyl−Dipeptides. *Adv. Mater.* **2006**, *18*, 611−614.

(19) Bieser, A. M.; Tiller, J. C. Supramolecular Self-Organization of Potential Hydrogelators on Attracting Surfaces. *Supramol. Chem.* **2008**, *20*, 363−367.

(20) Jadhav, R. S.; Vemula, P. K.; Kumar, R.; Raghavan, S. R.; John, G. Sugar-Derived Phase-Selective Molecular Gelators as Model Solidifiers for Oil Spills. *Angew. Chem., Int. Ed.* **2010**, *49*, 7695−7698.

(21) Bruns, N.; Tiller, J. C. Amphiphilic Network as Nanoreactor for Enzymes in Organic Solvents. *Nano Lett.* **2005**, *5*, 45−48.

(22) Dech, S.; Wruk, V.; Fik, C. P.; Tiller, J. C. Amphiphilic Polymer Co-networks Derived from Aqueous Solutions for Biocatalysis in Organic Solvents. *Polymer* **2012**, *53*, 701−707.

(23) Das, A. K.; Collins, R.; Ulijn, R. V. Exploiting Enzymatic (Reversed) Hydrolysis in Directed Self-Assembly of Peptide Nanostructures. *Small* **2008**, *4*, 279−287.
(24) George, M.; Weiss, R. G. Primary Alkyl Amines as Latent Gelators and Their Organogel Adducts with Neutral Triatomic Molecules. *Langmuir* **2003**, *19*, 1017−1025.
(25) *Molecular Gels, Materials with Self-Assembled Fibrillar Networks*; Weiss, R. G., Terech, P., Eds.; Springer: New York, 2006.
(26) Bag, B. G.; Dinda, S. K.; Dey, P. P.; Mallia, V. A.; Weiss, R. G. Self-Assembly of Esters of Arjunolic Acid into Fibrous Networks and the Properties of Their Organogels. *Langmuir* **2009**, *25*, 8663−8671.
(27) Geiger, C.; Stanescu, M.; Chen, L.; Whitten, D. G. Organogels Resulting from Competing Self-Assembly Units in the Gelator: Structure, Dynamics, and Photophysical Behavior of Gels Formed from Cholesterol−Stilbene and Cholesterol−Squaraine Gelators. *Langmuir* **1999**, *15*, 2241−2245.
(28) Terech, P.; Aymonier, C.; Loppinet-Serani, A.; Bhat, S.; Banerjee, S.; Das, R.; Maitra, U.; Del Guerzo, A.; Desvergne, J.-P. Structural Relationships in 2,3-Bis-*n*-decyloxyanthracene and 12-Hydroxystearic Acid Molecular Gels and Aerogels Processed in Supercritical CO_2. *J. Phys. Chem. B* **2010**, *114*, 11409−11419.
(29) Sangeetha, N. M.; Bhat, S.; Raffy, G.; Belin, C.; Loppinet-Serani, A.; Aymonier, C.; Terech, P.; Maitra, U.; Desvergne, J. P.; Guerzo, A. D. Hybrid Materials Combining Photoactive 2,3-DidecyloxyAnthracene Physical Gels and Gold Nanoparticles. *Chem. Mater.* **2009**, *21*, 3424−3432.
(30) Minkenberg, C. B.; Hendriksen, W. E.; Li, F.; Mendes, E.; Eelkema, R.; van Esch, J. H. Dynamic Covalent Assembly of Stimuli Responsive Vesicle Gels. *Chem. Commun.* **2012**, *48*, 9837−9839.
(31) Kar, T.; Debnath, S.; Das, D.; Shome, A.; Das, P. K. Organogelation and Hydrogelation of Low-Molecular-Weight Amphiphilic Dipeptides: pH-Responsiveness in Phase Selective Gelation and Dye Removal. *Langmuir* **2009**, *25*, 8639−8648.
(32) van de Manakker, F.; Braeckmans, K.; el Morabit, N.; De Smedt, S. C.; van Nostrum, C. F.; Hennink, W. E. Protein-Release Behavior of Self-Assembled PEG−*β*-Cyclodextrin/PEG−Cholesterol Hydrogels. *Adv. Funct. Mater.* **2009**, *19*, 2992−3001.
(33) Xue, P.; Lu, R.; Li, D.; Jin, M.; Bao, C.; Zhao, Y.; Wang, Z. Rearrangement of the Aggregation of the Gelator during Sol-Gel Transcription of a Dimeric Cholesterol-based Viologen Derivative into Fibrous Silica. *Chem. Mater.* **2004**, *16*, 3702−3707.
(34) Murata, K.; Aoki, M.; Nishi, T.; Ikeda, A.; Shinkai, S. New Cholesterol-based Gelators with Light- and Metal-Responsive Functions. *J. Chem. Soc., Chem. Commun.* **1991**, 1715−1718.
(35) Ajayaghosh, A.; Vijayakumar, C.; Varghese, R.; George, S. J. Cholesterol-Aided Supramolecular Control over Chromophore Packing: Twisted and Coiled Helices with Distinct Optical, Chiroptical, and Morphological Features. *Angew. Chem., Int. Ed.* **2006**, *45*, 456−460.
(36) Xue, M.; Gao, D.; Chen, X.; Liu, K.; Fang, Y. New Dimeric Cholesteryl-based $A(LS)_2$ Gelators with Remarkable Gelling Abilities: Organogel Formation at Room Temperature. *J. Colloid Interface Sci.* **2011**, *361*, 556−564.
(37) Svobodová, H.; Noponen, V.; Kolehmainen, E.; Sievänen, E. Recent Advances in Steroidal Supramolecular Gels. *RSC Adv.* **2012**, *2*, 4985−5007.
(38) Mitra, R. N.; Shome, A.; Paul, P.; Das, P. K. Antimicrobial Activity, Biocompatibility and Hydrogelation Ability of Dipeptide-based Amphiphiles. *Org. Biomol. Chem.* **2009**, *7*, 94−102.
(39) Roy, S.; Das, P. K. Antibacterial Hydrogels of Amino Acid-based Cationic Amphiphiles. *Biotechnol. Bioeng.* **2008**, *100*, 756−764.
(40) Haldar, J.; Kondaiah, P.; Bhattacharya, S. Synthesis and Antibacterial Properties of Novel Hydrolyzable Cationic Amphiphiles. Incorporation of Multiple Head Groups Leads to Impressive Antibacterial Activity. *J. Med. Chem.* **2005**, *48*, 3823−3831.
(41) Salick, D. A.; Kretsinger, J. K.; Pochan, D. J.; Schneider, J. P. Inherent Antibacterial Activity of a Peptide-based *β*-Hairpin Hydrogel. *J. Am. Chem. Soc.* **2007**, *129*, 14793−14799.
(42) Dutta, S.; Shome, A.; Kar, T.; Das, P. K. Counterion-Induced Modulation in the Antimicrobial Activity and Biocompatibility of Amphiphilic Hydrogelators: Influence of in situ Synthesized Ag-nanoparticle on the Bactericidal Property. *Langmuir* **2011**, *27*, 5000−5008.
(43) Das, D.; Kar, T.; Das, P. K. Gel-Nanocomposites: Materials with Promising Applications. *Soft Matter* **2012**, *8*, 2348−2365.
(44) Kubinová, S.; Horák, D.; Syková, E. Cholesterol-Modified Superporous Poly(2-hydroxyethyl methacrylate) Scaffolds for Tissue Engineering. *Biomaterials* **2009**, *30*, 4601−4609.
(45) Bhattarai, N.; Gunn, J.; Zhang, M. Chitosan-based Hydrogels for Controlled, Localized Drug Delivery. *Adv. Drug Delivery Rev.* **2010**, *62*, 83−99.
(46) Ahlstrom, B.; Chelminska-Bertilsson, M.; Thompson, R. A.; Edebo, L. Long-Chain Alkanoylcholines, a New Category of Soft Antimicrobial Agents That Are Enzymatically Degradable. *Antimicrob. Agents Chemother.* **1995**, *39*, 50−55.
(47) Salick, D. A.; Pochan, D. J.; Schneider, J. P. Design of an Injectable *β*-Hairpin Peptide Hydrogel That Kills Methicillin-Resistant Staphylococcus aureus. *Adv. Mater.* **2009**, *21*, 4120−4123.
(48) Das, D.; Maiti, S.; Brahmachari, S.; Das, P. K. Refining Hydrogelator Design: Soft Materials with Improved Gelation Ability, Biocompatibility and Matrix for in Situ Synthesis of Specific Shaped GNP. *Soft Matter* **2011**, *7*, 7291−7303.
(49) Roy, S.; Dasgupta, A.; Das, P. K. Alkyl Chain Length Dependent Hydrogelation of L-Tryptophan Based Amphiphile. *Langmuir* **2007**, *23*, 11769−11776.
(50) Brahmachari, S.; Das, D.; Das, P. K. Superior SWNT Dispersion by Amino Acid Based Amphiphiles: Designing Biocompatible Cationic Nanohybrids. *Chem. Commun.* **2010**, *46*, 8386−8388.
(51) Terech, P.; Dourdain, S.; Bhat, S.; Maitra, U. Self-Assembly of Bile Steroid Analogues: Molecules, Fibers, and Networks. *J. Phys. Chem. B* **2009**, *113*, 8252−8267.
(52) Debnath, S.; Shome, A.; Das, D.; Das, P. K. Hydrogelation through Self-Assembly of Fmoc-Peptide Functionalized Cationic Amphiphiles: Potent Antibacterial Agent. *J. Phys. Chem. B* **2010**, *114*, 4407−4415.
(53) Itagaki, H.; Fukiishi, H.; Imai, T.; Watase, M. Molecular Structure of Agarose Chains in Thermoreversible Hydrogels Revealed by Means of a Fluorescent Probe Technique. *J. Polym. Sci., Part B: Polym. Phys.* **2005**, *43*, 680−688.
(54) Clemente, M. J.; Fitremann, J.; Mauzac, M.; Serrano, J.; Oriol, L. Synthesis and Characterization of Maltose-based Amphiphiles as Supramolecular Hydrogelators. *Langmuir* **2011**, *27*, 15236−15247.
(55) Shome, A.; Dutta, S.; Maiti, S.; Das, P. K. In Situ Synthesized Ag Nanoparticle in Self-Assemblies of Amino Acid Based Amphiphilic Hydrogelators: Development of Antibacterial Soft Nanocomposites. *Soft Matter* **2011**, *7*, 3011−3022.
(56) Xing, B.; Yu, C.-W.; Chow, K.-H.; Ho, P.-L.; Fu, D.; Xu, B. Hydrophobic Interaction and Hydrogen Bonding Cooperatively Confer a Vancomycin Hydrogel: A Potential Candidate for Biomaterials. *J. Am. Chem. Soc.* **2002**, *124*, 14846−14847.
(57) Tiller, J. C. Increasing the Local Concentration of Drugs by Hydrogel Formation. *Angew. Chem., Int. Ed.* **2003**, *42*, 3072−3075.
(58) Mitra, R. N.; Das, P. K. In Situ Preparation of Gold Nanoparticles of Varying Shape in Molecular Hydrogel of Peptide Amphiphiles. *J. Phys. Chem. C* **2008**, *112*, 8159−8166.
(59) Vemula, P. K.; John, G. Smart Amphiphiles: Hydro/Organogelators for *in Situ* Reduction of Gold. *Chem. Commun.* **2006**, 2218−2220.
(60) Adhikari, B.; Banerjee, A. Short-Peptide-based Hydrogel: A Template for the in Situ Synthesis of Fluorescent Silver Nanoclusters by Using Sunlight. *Chem.—Eur. J.* **2010**, *16*, 13698−13705.
(61) Shrivastava, S.; Bera, T.; Roy, A.; Singh, G.; Ramachandrarao, P.; Dash, D. Characterization of Enhanced Antibacterial Effects of Novel Silver Nanoparticles. *Nanotechnology* **2007**, *18*, 225103 (9pp).